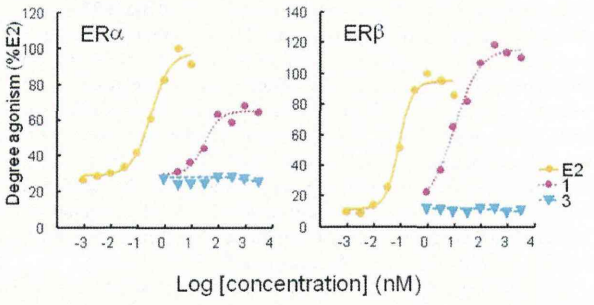

Figure 7. ER agonist potency of compounds **1** and **3** to nERs: dose dependence of binding of compounds **1** and **3** in HEK293h/ERα cells (left) or HEK293h/ERβ cells (right). Compound **1** showed dose-dependent agonist activity in both of HEK293/hERα cells (left) and HEK293/hERβ cells (right), though **3** showed no agonist potency for ERα or ERβ.

signal transduction pathways in a similar manner to estrogens.[29,30] However, we could not detect any effects of ICI182,780 alone on L-Glu transporter in our experiments (data not shown). In addition, Kuo et al. reported that GPR30 in astrocytes is detected not in the cell membranes but in the smooth endoplasmic reticulum,[31] while the cellular localization of GPR30 has been still controversially argued. In these contexts, GPR30 is an unlikely mediator to block the L-Glu transporters by the action of **3**.

According to Kisanga et al., the concentration of Tam in serum during conventional treatment for breast cancer (1−20 mg daily) is in the range from 20 to 225 nM.[32] Because **3** is more hydrophobic than Tam (the values of clogP for Tam and **3** are 7.56 and 9.70, respectively), it should exhibit greater permeability into the brain. Although other L-Glu transporter inhibitors, mainly L-Glu/aspartate analogues, are known, few of them have high brain transfer rates. Therefore, **3** is expected to be useful for biological research, and is also considered to be a promising candidate or lead compound for pharmacological application.

In conclusion, examination of several Tam-inspired compounds led to the discovery of two compounds that inhibited astrocytic L-Glu transporters at picomolar concentration. The inhibitory activity of compound **1** was mediated through the ER-MAPK/PI3K pathway, like that of Tam, though its transactivation activity was drastically reduced as compared with E2. In contrast, the inhibitory effect of **3** was manifested through an ER-independent and MAPK-independent, but PI3K-dependent pathway, and **3** showed no transactivation activity. These results suggest that **3** may represent a new platform for the development of novel L-Glu transporter inhibitors with higher brain transfer rates and reduced adverse effects.

METHODS

Chemistry. *General Procedures.* All reagents were commercial products and were used without further purification, unless otherwise noted. NMR data were recorded on a JEOL-400 or a Bruker Avance 400 NMR spectrometer (400 MHz for ^{1}H NMR and 100 MHz for ^{13}C NMR). *d*-$CDCl_3$ was used as a solvent, unless otherwise noted. Chemical shifts (δ) are reported in ppm with respect to internal tetramethylsilane (δ = 0 ppm) or undeuterated residual solvent (i.e., $CHCl_3$ (δ = 7.265 ppm)). Coupling constants are given in hertz. Coupling patterns are indicated as follows: m = multiplet, d = doublet, s = singlet, br = broad. High-resolution mass spectrometry (HRMS) was conducted in the electron spray ionization (ESI)-time-of-flight

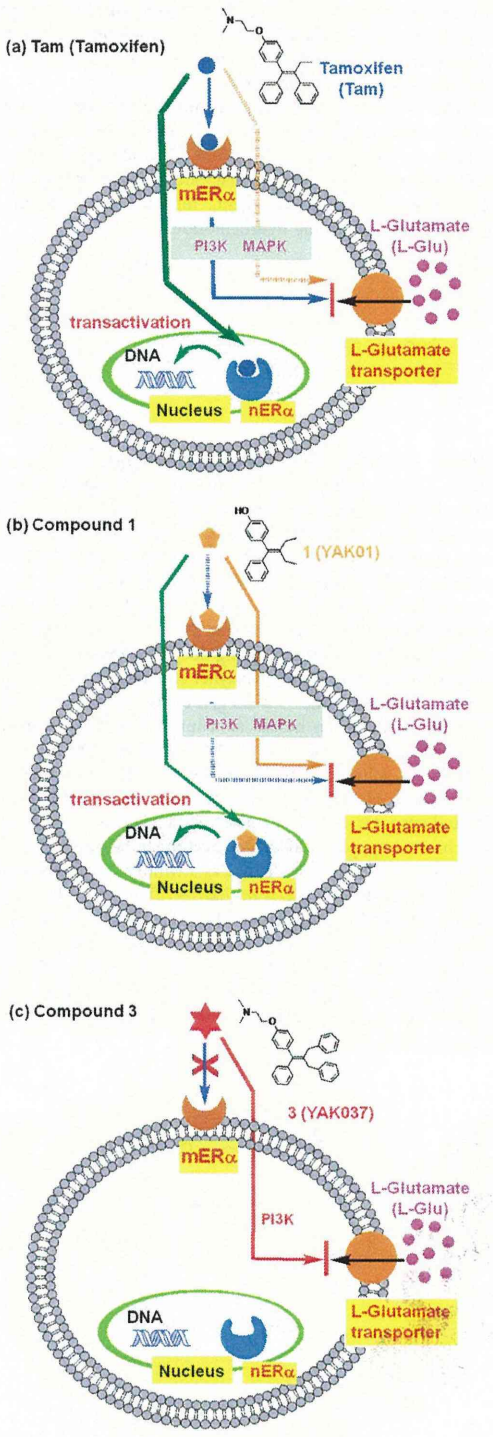

Figure 8. Schematic illustration of the proposed mechanisms of the effects of tamoxifen (a) and compounds **1** (b) and **3** (c).

(TOF) detection mode on a Bruker micrOTOF-05. FAB-MS and high-resolution FAB-MS were obtained on a JMS700-MSTATION (JEOL, Japan). Column chromatography was carried out on silica gel (silica gel 60N (100−210 mm), Kanto Chemicals, Japan). Flash column chromatography was performed on silica gel H (Merck, Germany). Analytical thin-layer chromatography (TLC) was performed on

dx.doi.org/10.1021/cn200091w | ACS Chem. Neurosci. XXXX, XXX, XXX−XXX

precoated plates of silica gel HF_{254} (Merck, Germany). All the melting points were measured with a Yanaco Micro Melting Point apparatus and are uncorrected. Combustion analyses were carried out in the microanalysis laboratory of this faculty.

Synthesis of Compounds. Compounds **1** and **2** were synthesized from 4-hydroxybenzophenone and butyl-3-one or dibenzylacetone by using $TiCl_4$ in the presence of $LiAlH_4$. Introduction of the *N,N*-dimethylaminoethyl moiety at the phenolic hydroxyl group of **1** and **2** was carried out by base treatment, followed by addition of 2-dimethylaminoethyl chloride hydrochloride.

2 (YAK050)

Synthesis of Tamoxifen-Related Compounds. Compound 2 (YAK050). To a suspension of Zn powder (916.6 mg; 6.9 equiv with respect to 4-hydroxybenzophenone) in dry THF (30 mL) in a 200 mL three-necked flask, $TiCl_4$ (0.61 mL, 2.8 equiv) was added dropwise under an argon atmosphere at −20 °C (in an ice-salt bath) over 2 min. The resulting light green-yellow mixture was stirred at −20 °C for 20 min and then the cooling bath was removed. After 20 min, the flask was immersed in a preheated oil bath at 100 °C and refluxed at 100 °C with stirring for 2.5 h. To the resulting deep blue mixture was added in one portion a solution of 4-hydroxybenzophenone (401.3 mg, 2.02 mmol) and dibenzyl ketone (1.2735 g, 3 equiv) in 50 mL of dry THF. The resultant mixture was heated at reflux at 100 °C with stirring for 2 h, then allowed to cool to rt, and poured into 400 mL of 0.5 N aqueous NaOH solution. The whole was extracted with ethyl acetate (500 mL). The organic layer was washed with water, dried over $MgSO_4$ and evaporated to give a pale yellow oil (1.5172 g), which was column-chromatographed (silica gel, acetone/*n*-hexane (1:7)) to give 365.0 mg (48% yield) of the olefin **2** as a white amorphous solid. Mp: 57–60 °C. ^1H NMR ($CDCl_3$): δ: 7.287–7.079 (m, 17H), 6.760 (d, 2H, J = 8.8 Hz), 4.792 (s, 1H), 3.413 (s, 2H), 3.377 (s, 2H). ^{13}C NMR ($CDCl_3$): δ: 154.1, 143.0, 140.7, 140.4, 135.8, 135.4, 130.7, 129.4, 128.8, 128.3, 128.3, 128.2, 126.5, 125.9, 115.1, 37.4, 37.2. HRMS (ESI^-): Calcd. for $C_{28}H_{23}O$ ($[M - H]^-$), 375.1754. Found: 375.1744. Anal. Calcd for $C_{28}H_{24}O{\cdot}0.2H_2O$: C, 88.48; H, 6.47; N, 0.00. Found: C, 88.36; H, 6.63; N, 0.00.

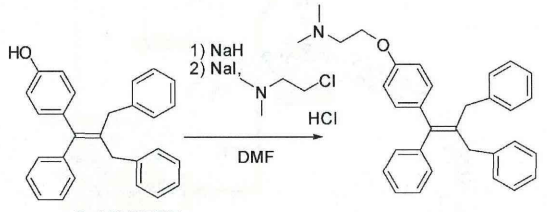

2 (YAK050)

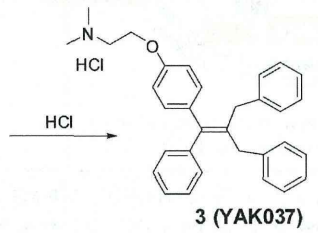

3 (YAK037)

Compound 3 (YAK037). To a suspension of NaH (60%, 42 mg, 1.05 mmol) in DMF (3 mL) at 0 °C was added a solution of the phenol **2** (158.2 mg, 0.420 mmol) in DMF (3 mL). The reaction mixture was stirred for 30 min at 0 °C, and then a solution of 2-dimethylaminoethyl chloride hydrochloride (181.0 mg, 1.256 mmol, 3.0 equiv) and NaI (94.0 mg, 0.627 mmol, 1.5 equiv) in DMF (3 mL) was added. The reaction mixture was stirred at 50 °C for 30 min, and then saturated aqueous NH_4Cl was added to quench the reaction. The mixture was extracted with Et_2O. The organic layer was washed with brine, dried over Na_2SO_4 and evaporated to afford a residue, which was column-chromatographed (ethyl acetate/Et_3N = 100/1) to give the intermediate amine (83.0 mg, 44% yield). The HCl salt of the resultant amine was prepared by repeated addition of a solution of 2 N HCl in Et_2O to a solution of the amine in ethyl acetate, followed by evaporation of the organic solvent to give **3**.

3: White solid. Mp. 169–170 °C. ^1H NMR ($CDCl_3$): δ: 13.073 (brs, 1H), 7.306–7.195 (m, 13H), 7.102–7.074 (m, 4H), 6.832 (d, 2H, J = 8.8 Hz), 4.481–4.459 (m, 2H), 3.425–3.390 (m, 6H), 2.893 (s, 6H). ^{13}C NMR ($CDCl_3$) δ: 155.7, 142.8, 140.4, 140.3, 140.2, 136.8, 136.2, 130.9, 129.4, 128.8, 128.7, 128.4, 128.3, 128.3, 126.6, 126.0, 125.9, 114.3, 62.8, 56.5, 43.6, 37.4, 37.2. HRMS (ESI^+, $[M + H]^+$): Calcd. for $C_{32}H_{34}NO$, 448.26349. Found: 448.26092. Anal. Calcd for $C_{32}H_{34}ClNO{\cdot}1/4H_2O$: C, 78.67; H, 7.12; N, 2.87. Found: C, 78.64; H, 7.30; N, 2.87.

Compound 1 (YAK01).

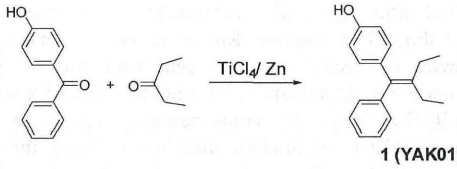

1 (YAK01)

To a suspension of Zn (0.86 g, 13.2 mmol) in 30 mL of dry THF at −5 °C was added dropwise $TiCl_4$ (0.72 mL, 6.6 mmol) under an argon atmosphere. The mixture was heated at reflux for 2 h. A solution of 4-hydroxybenzophenone (341.1 mg, 1.7 mmol) and 3-pentanone (0.50 mL, 5.0 mmol) in 50 mL of dry THF was added in one portion, and heating was continued at reflux for 6 h. Then the reaction mixture was cooled to rt, quenched with 10% aqueous K_2CO_3 (100 mL) and extracted with ethyl acetate (3 × 80 mL). The combined organic phase was washed with brine (50 mL), dried over Na_2SO_4, and evaporated to give a residue, which was flash column-chromatographed (3:1 hexane/ethyl acetate) to afford **1** (383.4 mg, 88.3%) as a white solid.

1: Mp. 76.0–76.5 °C (colorless needles, recrystallized from *n*-hexane). ^1H NMR ($CDCl_3$) δ: 7.261 (2H, t, J = 8.0 Hz), 7.173 (1H, d, J = 7.2 Hz), 7.128 (2H, d, J = 7.6 Hz), 7.009 (2H, d, J = 8.8 Hz), 6.726 (2H, d, J = 8.8 Hz), 4.763 (1H, s), 2.152 (2H, quartet, J = 7.6 Hz), 2.115 (2H, quartet, J = 6.0 Hz), 1.007 (3H, t, J = 7.6 Hz), 0.994 (3H, t, J = 7.6 Hz). ^{13}C NMR ($CDCl_3$) δ: 153.7, 143.7, 142.0, 136.5, 136.2, 130.5, 129.2, 127.9, 125.9, 114.8, 24.4, 24.3, 13.3. HRMS (ESI^-, $[M - H]^-$): Calcd. for $C_{18}H_{19}O^-$, 251.14414. Found: 251.14730. HRMS (FAB-MS, $[M]^+$) Calcd. for $C_{18}H_{20}O$, 252.1514. Found: 252.1528. Anal. Calcd. for $C_{18}H_{20}O$: C, 85.67; H, 7.99; N, 0.00. Found: C, 85.38; H, 8.13; N, 0.00.

Compound 4 (YAK06).

2-Dimethylaminoethyl chloride hydrochloride (282.4 mg, 2.0 mmol) and K_2CO_3 (1.5734 g, 11.4 mmol) were stirred in acetone/H_2O (18 mL/2 mL) at 0 °C for 30 min, then compound **1** (139.1 mg, 0.55 mmol) and K_2CO_3 (421.1 mg, 3.1 mmol) were added, and the whole was heated at reflux for 24 h, then cooled to rt. Inorganic materials were removed by filtration, and the filtrate was evaporated. The residue was flash column-chromatographed (100:1 ethyl acetate/Et_3N) to afford the amine as a white solid (88.0 mg). To a solution of the amine in ethyl acetate, a solution of HCl in ether was added to give a precipitate, which was collected and recrystallized from ethanol/ethyl acetate to give **4** (95.0 mg, 48%) as a white powder. **4**: Mp. 129.5–130.2 °C. ^1H NMR ($CDCl_3$) δ 726–6.90 (9H, m), 4.07 (2H, t, J = 6.0 Hz), 2.75 (2H, t, J = 6.0 Hz), 2.40 (6H, s), 2.15 (4H, d, J = 7.2 Hz), 1.00 (6H, t, J = 7.2 Hz). HRMS (FAB-MS, $[M\text{-}Cl]^+$): Calcd. for $C_{22}H_{30}NO^+$: 324.2322. Found: 324.2321.

dx.doi.org/10.1021/cn200091w | ACS Chem. Neurosci. XXXX, XXX, XXX–XXX

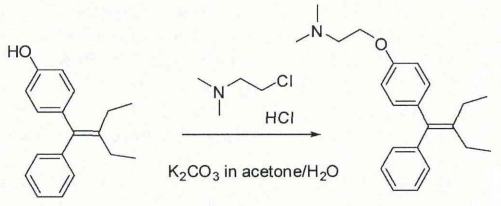

1 (YAK01)

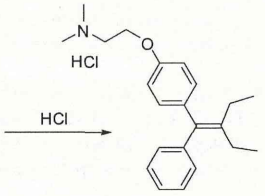

4 (YAK06)

Biology. All procedures using live animals in this study were conducted in accordance with the guidelines of the National Institute of Health Sciences, Japan.

Materials. Dulbecco's modified Eagle's medium (DMEM) and fetal bovine serum (FBS) were purchased from GIBCO (CA, USA). Glutamate dehydrogenase (GLD) was purchased from Roche (Mannheim, Germany). β-Nicotinamide adenine dinucleotide (βNAD), 3-(4,5-dimethyl-2-thiazolyl)-2,5-diphenyl-2H-tetrazolium bromide (MTT), 1-methoxy-5-methylphenazinium methyl sulfate (MPMS), lactate lithium salt and LY294002 were purchased from Sigma (MO, USA). DL-threo-β-benzyloxyaspartic acid (TBOA) and ICI182,780 were purchased from Tocris (MO, USA). U0126 was purchased from Promega (WI, USA). Assay kits for hormonal effects on HEK293/hERα and HEK293/hERβ reporter cells were purchased from Clontech (CA, USA).

Cell Culture. Primary cultures of astrocytes were prepared from the cerebral cortices of 3-day-old neonates of Wistar rats, as described previously.[14] Briefly, dissociated cortical cells were suspended in modified DMEM containing 30 mM glucose, 2 mM glutamine, 1 mM pyruvate and 10% FBS, and plated on uncoated 75 cm^2 flasks at the density of 600 000 cells/cm^2. A monolayer of type I astrocytes was obtained 12−14 days after plating. Nonastrocytes such as microglia were detached from the flasks by shaking and removed by changing the medium. Astrocytes in the flasks were dissociated by trypsinization, reseeded on uncoated 96-well microtiter plates at 20 000 cells/cm^2, and incubated until the cells became confluent (approximately 9−10 days after reseeding). In this culture, >98% of the cells were identified as type I astrocytes on the basis of positivity for GFAP and flattened, polygonal appearance.

Measurement of Extracellular L-Glu Concentration. Extracellular L-Glu concentration was measured by means of a colorimetric method according to Abe et al.[15] Briefly, 50 μL of culture supernatant was transferred to each well of a 96-well microtiter plate and mixed with 50 μL of substrate mixture consisting of 20 U/mL GLD, 2.5 mg/mL β-NAD, 0.25 mg/mL MTT, 100 μM MPMS and 0.1% (v/v) Triton X-100 in 0.2 M Tris-HCl buffer (pH 8.2). After 10 min incubation at 37 °C, the reaction was stopped by adding 100 μL of solution containing 50% (v/v) dimethylformamide and 20% (wt/vol) SDS (pH 4.7). In this reaction, MTT (yellow) is converted into MTT formazan (purple) in proportion to the L-Glu concentration. The amount of MTT formazan was determined by measuring the absorbance at 570 nm (test wavelength) and 655 nm (reference wavelength) with a microplate reader. The concentration of L-Glu was estimated from a standard curve, which was constructed in each assay using cell-free medium containing known concentrations of L-Glu. L-Glu clearance was shown as the amount of L-Glu taken up by astrocytes, which was calculated from the concentration difference in the medium.

Treatment with Test Compounds. L-Glu was dissolved at 1 mM in phosphate-buffered saline and diluted to 100 μM with the culture medium. Compounds **1**, **2**, **3**, and **4** were dissolved at 100, 100, 100, and 10 mM, respectively, in dimethyl sulfoxide (DMSO) and diluted to the required final concentrations with the culture medium. The concentration of DMSO in the medium was controlled to be below 0.1%, because we had already confirmed that 0.1% DMSO has no effect on L-Glu transport activity or cell viability (data not shown). Cells were incubated with test compounds for 24 h. TBOA (IC50 = 48 μM for GLAST, 7 μM for GLT1) was freshly dissolved at 1 mM in culture medium for each experiment. ICI182,780 (IC50 = 0.29 nM for ERs), U0126 (IC50 = 72 nM for MEK1, 58 nM for MEK2), and LY294002 (IC50 = 1 μM for class 1 PI3K, 19 μM for class 2 PI3K) were dissolved at 1, 5, and 5 mM, respectively, in DMSO, and the solutions were diluted with culture medium to yield the required final concentrations. These inhibitors were coapplied with 1 nM test compounds (**1**−**4**) for 24 h.

Assay Procedure for Hormonal Effects on HEK293/hERα and HEK293/hERβ Reporter Cells. Human embryo kidney 293 cells (HEK293) were grown in FBS (+) DMEM in 100 mm dishes. Cells were subcultured once or twice a week at about 80% confluence. A solution of 12.4 μL of 2 M calcium ion, 100 ng/well reporter or negative control vector (pERE-TA-SEAP or pTA-SEAP, Clontech), 50 ng/well expression vector (pcDNA3 ERα or pcDNA3 ERβ, generous gift from Dr. Shige-aki Kato, University of Tokyo, Japan), and 100 ng/well positive control vector (pSV-β-galactosidase, Promega) was diluted to a final volume of 10 μL/well. This mixture was carefully added dropwise to the same volume of HEPES solution with slow vortexing, and the mixture was incubated at rt for 20 min to obtain a precipitate. Cells from the exponential growth phase were seeded (3.0 × 10^4 cells/ml) into 96-well plates the day before transfection. The cells were incubated with fresh medium for 1 h, then 1/10 volume of precipitate was added to each well and incubation was continued for 24 h at 37 °C in an atmosphere of 5% CO_2 in air. The medium was replaced with fresh FBS (-) medium and incubation was continued for a further 24 h. Then the cells were incubated with test compounds for 24 h at 37 °C in an atmosphere of 5% CO_2 in air. SEAP activity (Great EscapeTM SEAP chemiluminescence kit 2.0, Clontech) and β-galactosidase activity (β-Galactosidase Enzyme Assay System with Reporter Lysis Buffer, Promega) were measured with a Spectramax M5 microplate reader (Molecular Devices Japan, Tokyo, Japan). All transfections were performed in triplicate.

Statistical Analysis. Data were obtained from four independent experiments (averaged values of six wells for each) unless otherwise noted. Data are expressed as means ± SEM of these data. Tests of homogeneity of variance, normality, and distribution were performed to ensure that the assumptions required for standard parametric ANOVA were satisfied. Statistical analysis was performed by one-way repeated-measures ANOVA with post hoc Tukey's test for multiple pairwise comparisons.

■ AUTHOR INFORMATION

Corresponding Author

*(K.S.) Telephone and Fax: +81-3-3700-9698. E-mail: kasato@nihs.go.jp. (T.O.) Telephone: +81-3-5840-4730. Fax: +81-3-5840-4735. E-mail: ohwada@mol.f.u-tokyo.ac.jp.

Author Contributions

†These two authors equally contributed to this Article.

Funding

This work was partly supported by a Grant-in-Aid from the Food Safety Commission, Japan (No. 1003), a Grant-in-Aid for Young Scientists from MEXT, Japan (KAKENHI 21700422), the Program for Promotion of Fundamental Studies in Health Sciences of NIBIO, Japan, a Health and Labor Science Research Grant for Research on Risks of Chemicals, a Health and Labor Science Research Grant for Research on New Drug Development from MHLW, Japan, awarded to K.S., and a Health and Labor Science Research Grant for Research on Risks of Chemicals from MHLW, Japan, awarded to K.N. and T.O.

dx.doi.org/10.1021/cn200091w | ACS Chem. Neurosci. XXXX, XXX, XXX−XXX

Notes

The authors declare no competing financial interest.

■ ACKNOWLEDGMENTS

We thank Dr. Shige-aki Kato for providing pcDNA3 hERα and pcDNA3 hERβ.

■ ABBREVIATIONS

βNAD; β-nicotinamide adenine dinucleotide; CNS; central nervous system; DMEM; Dulbecco's modified Eagle's medium; DMSO; dimethyl sulfoxide; E2; 17β-estradiol; ESI; electron spray ionization; FBS; fetal bovine serum; GLD; glutamate dehydrogenase; HEK-293; Human embryo kidney 293 cells; HRMS; high-resolution mass spectrometry; L-Glu; L-glutamate; MAPK; mitogen-activated protein kinase; MEK; mitogen-activated protein kinase/extracellular signal-regulated kinase; mERα; membrane-associated estrogen receptor α; mGluR5; metabotropic glutamate receptor 5; MPMS; 1-methoxy-5-methylphenazinium methyl sulfate; MTT; 3-(4,5-dimethyl-2-thiazolyl)-2,5-diphenyl-2H-tetrazolium bromide; nERs; nuclear estrogen receptors; PI3K; phosphatidylinositol 3-kinase; Tam; tamoxifen; TBOA; DL-threo-β-benzyloxyaspartic acid; TLC; thin-layer chromatography; TOF; time-of-flight

■ REFERENCES

(1) Kumar, A., Singh, R. L., and Babu, G. N. (2010) Cell death mechanisms in the early stages of acute glutamate neurotoxicity. *Neurosci. Res. 66*, 271–278.

(2) Choi, D. W. (1988) Glutamate neurotoxicity and diseases of the nervous system. *Neuron 1*, 623–634.

(3) Logan, W. J., and Snyder, S. H. (1971) Unique high affinity uptake systems for glycine, glutamic and aspartic acids in central nervous tissue of the rat. *Nature 234*, 297–299.

(4) Beart, P. M., and O'Shea, R. D. (2007) Transporters for L-glutamate: an update on their molecular pharmacology and pathological involvement. *Br. J. Pharmacol. 150*, 5–17.

(5) Sato, K., Matsuki, N., Ohno, Y., and Nakazawa, K. (2003) Estrogens inhibit L-glutamate uptake activity of astrocytes via membrane estrogen receptor alpha. *J. Neurochem. 86*, 1498–1505.

(6) Olivier, S., Close, P., Castermans, E., de Leval, L., Tabruyn, S., Chariot, A., Malaise, M., Merville, M. P., Bours, V., and Franchimont, N. (2006) Raloxifene-induced myeloma cell apoptosis: a study of nuclear factor-kappaB inhibition and gene expression signature. *Mol. Pharmacol. 69*, 1615–1623.

(7) Sato, K., Saito, Y., Oka, J., Ohwada, T., and Nakazawa, K. (2008) Effects of tamoxifen on L-glutamate transporters of astrocytes. *J. Pharmacol. Sci. 107*, 226–230.

(8) Bunch, L., Erichsen, M. N., and Jensen, A. A. (2009) Excitatory amino acid transporters as potential drug targets. *Expert Opin. Ther. Targets 13*, 719–731.

(9) Margueron, R., Duong, V., Bonnet, S., Escande, A., Vignon, F., Balaguer, P., and Cavailles, V. (2004) Histone deacetylase inhibition and estrogen receptor alpha levels modulate the transcriptional activity of partial antiestrogens. *J. Mol. Endocrinol. 32*, 583–594.

(10) Thompson, D. S., Spanier, C. A., and Vogel, V. G. (1999) The relationship between tamoxifen, estrogen, and depressive symptoms. *Breast J. 5*, 375–382.

(11) Grilli, S. (2006) Tamoxifen (TAM): the dispute goes on. *Ann. Ist. Super. Sanita 42*, 170–173.

(12) Sha, Y., Tashima, T., Mochizuki, Y., Toriumi, Y., Adachi-Akahane, S., Nonomura, T., Cheng, M., and Ohwada, T. (2005) Compounds structurally related to tamoxifen as openers of large-conductance calcium-activated K^+ channel. *Chem. Pharm. Bull. (Tokyo) 53*, 1372–1373.

(13) Robertson, D. W., Katzenellenbogen, J. A., Long, D. J., Rorke, E. A., and Katzenellenbogen, B. S. (1982) Tamoxifen antiestrogens. A comparison of the activity, pharmacokinetics, and metabolic activation of the cis and trans isomers of tamoxifen. *J. Steroid Biochem. 16*, 1–13.

(14) Suzuki, K., Ikegaya, Y., Matsuura, S., Kanai, Y., Endou, H., and Matsuki, N. (2001) Transient upregulation of the glial L-glutamate transporter GLAST in response to fibroblast growth factor, insulin-like growth factor and epidermal growth factor in cultured astrocytes. *J. Cell Sci. 114*, 3717–3725.

(15) Abe, K., Abe, Y., and Saito, H. (2000) Evaluation of L-glutamate clearance capacity of cultured rat cortical astrocytes. *Biol. Pharm. Bull. 23*, 204–207.

(16) Weltje, L., vom Saal, F. S., and Oehlmann, J. (2005) Reproductive stimulation by low doses of xenoestrogens contrasts with the view of hormesis as an adaptive response. *Hum. Exp. Toxicol. 24* (9), 431–437.

(17) Perego, C., Vanoni, C., Bossi, M., Massari, S., Basudev, H., Longhi, R., and Pietrini, G. (2000) The GLT-1 and GLAST glutamate transporters are expressed on morphologically distinct astrocytes and regulated by neuronal activity in primary hippocampal co-cultures. *J. Neurochem. 75*, 1076–1084.

(18) Guillet, B., Lortet, S., Masmejean, F., Samuel, D., Nieoullon, A., and Pisano, P. (2002) Developmental expression and activity of high affinity glutamate transporters in rat cortical primary cultures. *Neurochem. Int. 40*, 661–671.

(19) Razandi, M., Pedram, A., Greene, G. L., and Levin, E. R. (1999) Cell membrane and nuclear estrogen receptors (ERs) originate from a single transcript: studies of ERalpha and ERbeta expressed in Chinese hamster ovary cells. *Mol. Endocrinol. 13*, 307–319.

(20) Pappas, T. C., Gametchu, B., and Watson, C. S. (1995) Membrane estrogen receptors identified by multiple antibody labeling and impeded-ligand binding. *FASEB J. 9*, 404–410.

(21) Grove-Strawser, D., Boulware, M. I., and Mermelstein, P. G. (2010) Membrane estrogen receptors activate the metabotropic glutamate receptors mGluR5 and mGluR3 to bidirectionally regulate CREB phosphorylation in female rat striatal neurons. *Neuroscience 170*, 1045–1055.

(22) Mannella, P., and Brinton, R. D. (2006) Estrogen receptor protein interaction with phosphatidylinositol 3-kinase leads to activation of phosphorylated Akt and extracellular signal-regulated kinase 1/2 in the same population of cortical neurons: a unified mechanism of estrogen action. *J. Neurosci. 26*, 9439–9447.

(23) Szego, E. M., Barabas, K., Balog, J., Szilagyi, N., Korach, K. S., Juhasz, G., and Abraham, I. M. (2006) Estrogen induces estrogen receptor alpha-dependent cAMP response element-binding protein phosphorylation via mitogen activated protein kinase pathway in basal forebrain cholinergic neurons ~~in vivo~~. *J. Neurosci. 26*, 4104–4110.

(24) Vasudevan, N., Kow, L. M., and Pfaff, D. (2005) Integration of steroid hormone initiated membrane action to genomic function in the brain. *Steroids 70*, 388–396.

(25) Alyea, R. A., Laurence, S. E., Kim, S. H., Katzenellenbogen, B. S., Katzenellenbogen, J. A., and Watson, C. S. (2008) The roles of membrane estrogen receptor subtypes in modulating dopamine transporters in PC-12 cells. *J. Neurochem. 106* (4), 1525–1533.

(26) Watson, C. S., Alyea, R. A., Hawkins, B. E., Thomas, M. L., Cunningham, K. A., and Jakubas, A. A. (2006) Estradiol effects on the dopamine transporter - protein levels, subcellular location, and function. *J. Mol. Signaling 1*, 5.

(27) Filardo, E. J., and Thomas, P. (2005) GPR30: a seven-transmembrane-spanning estrogen receptor that triggers EGF release. *Trends. Endocrinol. Metab. 16* (8), 362–367.

(28) Revankar, C. M., Cimino, D. F., Sklar, L. A., Arterburn, J. B., and Prossnitz, E. R. (2005) A transmembrane intracellular estrogen receptor mediates rapid cell signaling. *Science 11;307* (5715), 1625–1630.

(29) Filardo, E. J., Quinn, J. A., Bland, K. I., and Frackelton, A. R. Jr. (2000) Estrogen-induced activation of Erk-1 and Erk-2 requires the G protein-coupled receptor homolog, GPR30, and occurs via trans-activation of the epidermal growth factor receptor through release of HB-EGF. *Mol. Endocrinol. 14* (10), 1649–1660.

dx.doi.org/10.1021/cn200091w | *ACS Chem. Neurosci.* XXXX, XXX, XXX–XXX

(30) Thomas, P., Pang, Y., Filardo, E. J., and Dong, J. (2005) Identity of an estrogen membrane receptor coupled to a G protein in human breast cancer cells. *Endocrinology 146* (2), 624–632.
(31) Kuo, J., Hamid, N., Bondar, G., Prossnitz, E. R., and Micevych, P. (2010) Membrane estrogen receptors stimulate intracellular calcium release and progesterone synthesis in hypothalamic astrocytes. *J. Neurosci. 30* (39), 12950–12957.
(32) Kisanga, E. R., Gjerde, J., Guerrieri-Gonzaga, A., Pigatto, F., Pesci-Feltri, A., Robertson, C., Serrano, D., Pelosi, G., Decensi, A., and Lien, E. A. (2004) Tamoxifen and metabolite concentrations in serum and breast cancer tissue during three dose regimens in a randomized preoperative trial. *Clin. Cancer Res. 10*, 2336–2343.

dx.doi.org/10.1021/cn200091w | *ACS Chem. Neurosci.* XXXX, XXX, XXX–XXX

SCIENTIFIC REPORTS

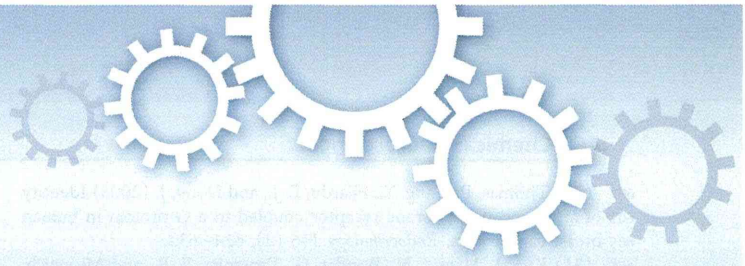

OPEN

SUBJECT AREAS:
INDUCED PLURIPOTENT STEM CELLS
EMBRYONIC STEM CELLS

Received
9 October 2013

Accepted
6 December 2013

Published
8 January 2014

Correspondence and requests for materials should be addressed to M.N. (nakagawa-g@cira.kyoto-u.ac.jp)

A novel efficient feeder-free culture system for the derivation of human induced pluripotent stem cells

Masato Nakagawa[1], Yukimasa Taniguchi[2], Sho Senda[3], Nanako Takizawa[1], Tomoko Ichisaka[1], Kanako Asano[1], Asuka Morizane[1], Daisuke Doi[1], Jun Takahashi[1], Masatoshi Nishizawa[1], Yoshinori Yoshida[1], Taro Toyoda[1], Kenji Osafune[1], Kiyotoshi Sekiguchi[2] & Shinya Yamanaka[1,4]

[1]Center for iPS Cell Research and Application (CiRA), Kyoto University, Kyoto 606-8507, Japan, [2]Institute for Protein Research, Osaka University, Osaka 565-0871, Japan, [3]Institute for Innovation, Ajinomoto CO., Inc., Kawasaki, 210-8681 Japan, [4]Gladstone Institute of Cardiovascular Disease, San Francisco, CA 94158 USA.

In order to apply human embryonic stem cells (hESCs) and induced pluripotent stem cells (hiPSCs) to regenerative medicine, the cells should be produced under restricted conditions conforming to GMP guidelines. Since the conventional culture system has some issues that need to be addressed to achieve this goal, we developed a novel culture system. We found that recombinant laminin-511 E8 fragments are useful matrices for maintaining hESCs and hiPSCs when used in combination with a completely xeno-free (Xf) medium, StemFit™. Using this system, hESCs and hiPSCs can be easily and stably passaged by dissociating the cells into single cells for long periods, without any karyotype abnormalities. Human iPSCs could be generated under feeder-free (Ff) and Xf culture systems from human primary fibroblasts and blood cells, and they possessed differentiation abilities. These results indicate that hiPSCs can be generated and maintained under this novel Ff and Xf culture system.

Human embryonic stem cells (hESCs) and induced pluripotent stem cells (hiPSCs) hold promise as tools for regenerative medicine. Recently, several reports have discussed the potential use of stem cells in clinical applications. Geron has initiated treatment of neural disease using neuronal cells derived from hESCs. Advanced Cell Technologies is making efforts to treat eye diseases with ESC-derived cells[1]. This approach involves the production of retinal pigment epithelium from hESCs that are then transplanted into patients. Regenerative medicine using stem cells, particularly pluripotent stem cells, will certainly advance over the coming years as new discoveries are made.

Researchers usually use feeder cells and serum-containing medium in conventional culture systems for hESCs and hiPSCs[2,3]. Murine-derived feeder cells are widely used to maintain hESCs and hiPSCs. Human-derived feeder cells are also used for hESC/iPSC culture; however, in some cases, these cells have proven unsuitable for stem cell maintenance[4,5]. The feeder cell preparation requires significant time and effort. Fetal bovine serum (FBS)-containing medium is normally used for the culture of feeder cells. The reduction or complete removal of serum and animal-derived products is required to satisfy Standard for Biological Ingredients. Moving towards feeder-free culture systems for hESCs and hiPSCs would represent a significant improvement over conventional culture systems.

To address these issues, we sought to develop a novel culture system applicable for human stem cell maintenance and hiPSC derivation. Feeder-free (Ff) and xeno-free (Xf) conditions appear to be acceptable for culturing hESCs and hiPSCs. Various matrices can be used to replace feeder cells, such as Matrigel[6–8], CELLstart[9,10], recombinant proteins[11–13] and synthetic polymers[14,15]. Xeno-free media are also available commercially, including TeSR2, NutriStem and Essential E8 medium[13], among others. Although we examined most of these materials with respect to whether the hESCs and hiPSCs could be stably and efficiently cultivated in our laboratory, we were unable to identify an efficacious combination of matrix and medium.

It has previously been reported that laminin-511 supports the stable culture of hESCs and hiPSCs[11]. Recently, a shorter fragment of laminin-511, referred to as the laminin-511 E8 fragment (LN511E8), was also shown to efficiently maintain hESCs and hiPSCs[12]. Recombinantly expressed LN511E8 (rLN511E8) is isolated more easily, and with a greater yield and purity, than full-length laminin-511. For these reasons, we chose rLN511E8 as a

matrix for our novel culture system for hESCs and hiPSCs. Next, we examined whether a new xeno-free medium, StemFit™, could be used for our novel culture system with rLN511E8.

Employing these materials, we successfully developed a novel culture system for hESCs and hiPSCs using rLN511E8 and StemFit™ that is easy to use, expandable and reproducible, as clinical-grade hiPSCs must be manufactured according to Standard Operating Procedures (SOPs) in order to meet Cell Processing Center (CPC) standards.

Human ESCs and iPSCs were stably passaged for long periods by dissociating the cells into single cells. Moreover, hiPSCs were successfully established from primary fibroblasts, peripheral blood and cord blood under these conditions using episomal vectors[16,17]. These Ff-hiPSCs displayed the capacity to differentiate into various types of somatic cells, including all three germ layers. These results indicate that Ff-hiPSCs are suitable for manufacturing in a CPC setting, and should prove useful for future research and clinical applications.

Results

Development of a novel culture system for hiPSCs. To develop feeder-free (Ff) and xeno-free (Xf) hiPSC culture conditions, we tested Matrigel, CellStart and the recombinant laminin-511 E8 fragment (rLN511E8) as coating matrices[12]. H9 hESCs were dissociated into single cells and plated onto the coated culture plates. The hESCs efficiently formed colonies on rLN511E8 but not on the other matrices (Figure S1A). We therefore selected rLN511E8 as the coating matrix for our system. Using rLN511E8, we attempted to cultivate hiPSCs using a variety of commercially available Xf-medium (Figure S1B). TeSR2 did not support the maintenance of hiPSCs (32R1[18]) on rLN511E8. When we used NutriStem, the hiPSCs formed flattened colonies. Although the mixture of TeSR2 and NutriStem supported hESC-like colony formation, the morphology was not good (many granules were detected in cells). Since we were unable to obtain good results, we chose to try StemFit™, a newly developed Xf-medium for hiPSC culture from Ajinomoto Co., Inc. Using StemFit™, we obtained hiPSCs colonies similar to those cultivated on feeder cells[2] (Figure S1B).

We examined whether hESCs and hiPSCs, which were previously established and maintained on feeder cells, can be cultivated under the Ff and Xf conditions using rLN511E8 matrix and StemFit™ (Figure 1A). After two or three passages, most of the hESCs and hiPSCs adapted to the Ff and Xf culture conditions. The combination of rLN511E8 and StemFit™ demonstrated efficacy for the hESCs and hiPSC culture.

Human iPSCs were then dissociated into single cells and reproducibly plated according to the exact cell number (Figure S2A), an important consideration for standardizing culture conditions and developing a reliable experimental design. The cells cultured on rLN-511E8 became confluent within 8–10 days after plating (the average fold change was 132 in each passage (Figure S2B)). The average doubling time was 28.34 hours (Figure S2B). This period was faster than that of hiPSCs cultivated on feeder cells[2]. Surprisingly, the high cell viability permitted a split ratio of nearly 1:100 (Figure S2B). Frozen stocks were prepared at −80°C using a standard slow-freezing method, and were thawed in a 37°C water bath (Figure S2A).

We next examined whether the hES/iPSCs could be stably cultivated over long periods using the new culture conditions. We used H9 hESCs, KhES1 hESCs and 201B7 hiPSCs for this experiment. The cells were stably maintained for 20–30 passages, and markers of pluripotency, such as Oct3/4 and TRA-1-60, were still detected (Figures 1B and 1C). Passage number 54 of the 201B7 cells still exhibited the ability to differentiate into all three germ layers *in vitro* (Figure S2C). We concluded that our method is sufficient and efficient for hESC and hiPSC culture. This culture system has already been tested and showed similar results at several other laboratories in Japan.

Establishment of hiPSCs under Ff and Xf conditions. Although we successfully developed a highly efficient system for the culture of hESCs and hiPSCs using rLN511E8 and StemFit™, hiPSCs intended for clinical application should be generated under similar conditions. First, we attempted to establish hiPSCs from human primary fibroblasts. Skin tissues were collected using biopsies, and fibroblasts were generated from the skin tissues. Fibroblasts were established under Xf conditions with medium containing 10% autologous serum. The fibroblasts were electroporated with episomal vectors containing reprogramming factors. Twenty to thirty days after electroporation, hiPSC colonies were observed and selected to establish feeder-free hiPSC (Ff-hiPSC) clones, 987A3 and 987A7 (Figure 2A). The morphology of the fibroblast-derived Ff-hiPSCs was similar to that of 201B7 or H9 cells cultivated on rLN511E8. The loss of episomal vectors was confirmed using a genomic PCR analysis (Figure S3A).

The expression levels of markers of pluripotency were examined using RT-PCR and immunostaining. The fibroblast-derived Ff-hiPSC clones exhibited similar expression levels to those of 201B7 and H9 cells (Figures 2B and S3B). The expression levels of genes related to pluripotency were similar in the cells cultivated on rLN511E8 and feeder cells (Figure 2B). The fibroblast-derived Ff-hiPSCs were stably passaged for long periods (Figure 2C) and had normal karyotypes (Figure S3C).

Ff-hiPSCs were also established from peripheral blood-derived T-cells, non-T-cells and cord blood. The morphology, marker gene expression levels and stability for long-term culture of these cells were similar to those of fibroblast-derived Ff-hiPSCs (Figures 2 and S3D).

The efficiency of Ff-hiPSC generation is summarized in Supplemental Table 1.

Differentiation capacity of Ff-hiPSCs. We examined whether Ff-hiPSCs have the ability to differentiate into several types of somatic cells. First, Ff-hiPSCs were cultivated on rLN511E8 with StemFit™ in the absence of bFGF. The cells efficiently attached to rLN511E8-coated plates and grew, exhibiting spontaneous differentiation. Two weeks after differentiation, we confirmed the expression levels of Sox17, α-smooth muscle actin (SMA) and βIII tubulin by immunostaining (Figure S4). Ff-hiPSCs were able to differentiate into all three germ layers *in vitro*. Moreover, in the teratoma assays, Ff-hiPSCs differentiated into various tissues of the three germ layers, including gut-like epithelial tissue, cartilage and neural tissue (Figure 3A). Another three Ff-hiPSC clones were also tested for the teratoma assays. These results demonstrated that the Ff-hiPSCs are functionally equivalent to iPSCs derived under feeder conditions[2], and have the potential to spontaneously differentiate into all three germ layers both *in vitro* and *in vivo*.

The directed differentiation of hiPSCs has the potential to generate various somatic cells for disease modeling, drug discovery, toxicology, prediction of side effects, and eventually, transplantation therapy. Therefore, we next examined whether Ff-hiPSCs could be specifically induced to differentiate towards somatic cells of therapeutic interest.

Parkinson's disease is characterized by the loss of dopaminergic (DA) neurons; therefore, hiPSC-derived DA neurons may be good sources for cell transplant therapy. Mature and functional DA neurons have been produced through long-term culture of hiPSCs on Matrigel[19]. We subjected Ff-hiPSCs to the neuronal differentiation protocol with dual SMAD inhibition. Consequently, the Ff-hiPSCs differentiated into DA neurons expressing tyrosine hydroxylase (TH), βIII tubulin (Tuj1), Nurr1 and Foxa2 (Figure 3B). This experiment was performed under Xf conditions. Therefore, these results indicate that DA neurons can be successfully generated under Xf conditions from human tissue samples obtained using Ff-hiPSCs cultured without Matrigel.

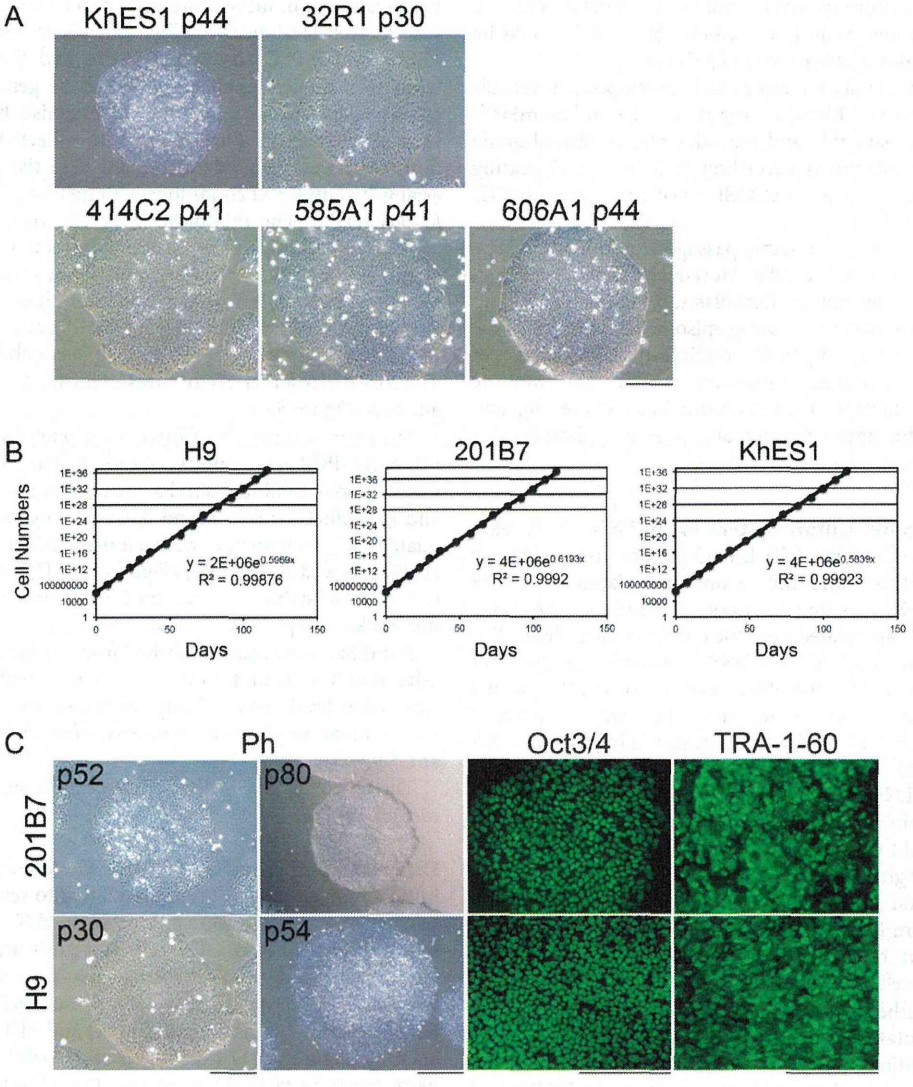

Figure 1 | The feeder-free (Ff) and xeno-free (Xf) culture system for hES/iPS cells. (A) The morphology of hESCs (KhES1) and hiPSCs (32R1, 414C2[31], 585A1[31] and 606A1[31]) cultivated on rLN511E8-coated cell culture plates with StemFit™. Scale bar, 100 μm. (B) The growth curves of the hESCs (H9 and KhES1) and hiPSCs (201B7) cultured under Ff and Xf conditions. Each dot represents a passage of cells. (C) The morphology of the indicated passage numbers of 201B7 and H9 cells. The 201B7 and H9 cells at passage numbers p80 and p54, respectively, were immunostained for the indicated pluripotency markers, followed by phase contrast imaging (Ph). Scale bar, 100 μm.

As a second target lineage with therapeutic potential, we chose to differentiate Ff-hiPSC into blood cells. Ff-hiPSCs were cultivated in a low-binding cell culture plate to promote the formation of EB-like spheres, which were sequentially treated with cytokines to invoke blood cell differentiation, as described previously[20]. Erythroblasts, macrophages and myeloid lineage cells were produced from Ff-hiPSCs, as demonstrated using May-Grunwald-Giemsa staining (Figure 3C).

The third target cells induced were insulin-producing cells. The differentiation of Ff-hiPSCs into insulin-producing cells has been reported previously[21], and we made use of a similar protocol. Consequently, insulin-producing cells were generated from Ff-hiPSCs (Figure 3D). These results indicate that Ff-hiPSCs cultured under Xf conditions have the ability to differentiate into specific cells of interest using established *in vitro* induction protocols, with some minor modifications to maintain the Xf conditions. The efficiency and quality should be examined by the future experiments.

Discussion

We developed a novel efficient culture system for hES/iPSCs without feeder cells. Recombinant LN511E8 strongly supported hESC and hiPSC culture for long periods. StemFit™, a newly developed Xf-medium, was the best medium for hESC and hiPSC culture with rLN511E8. Under this novel culture system, hESCs and hiPSCs were passaged by dissociating them into single cells. Moreover, hESC and hiPSCs could be cryopreserved at −80°C by the slow-freezing method. Ff-hiPSCs showed the ability to differentiate into several somatic cell types, similar to conventional hiPSCs cultured on feeder cells[2].

The culture system using rLN511E8 has been reported previously by Miyazaki et al.[12]. The authors also passaged hES/iPSCs by dissociating into single cells. Despite the basic idea is the same, we could develop more efficient method using StemFit™, achieving significantly better attachment efficiency at 6 hours after plating (Supplementary Table 2). Moreover, we confirmed the requirement of the glutamic acid residue in the C-terminal tail of the laminin γ1

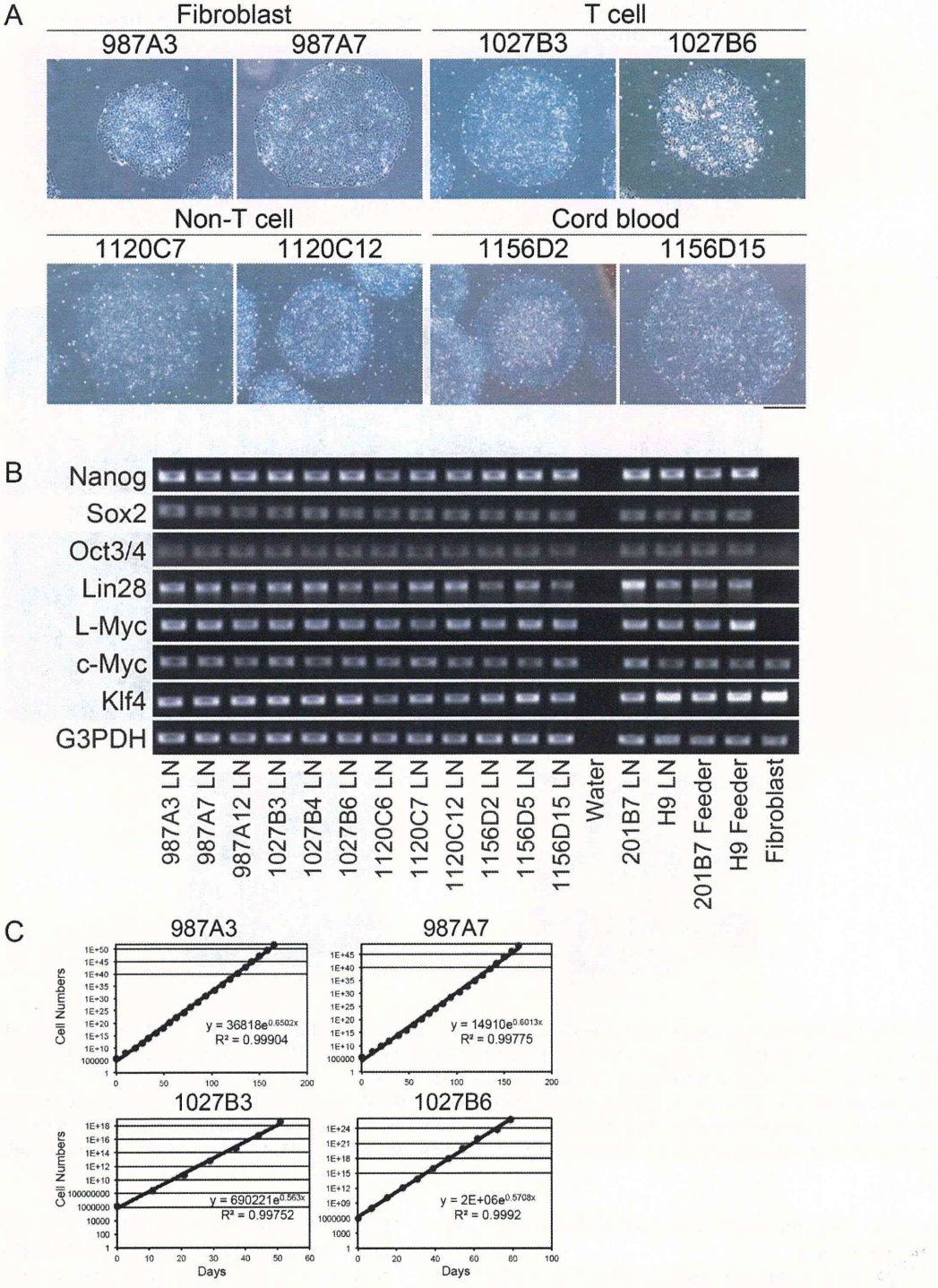

Figure 2 | Establishment of iPS cell clones under the feeder-free (Ff) and xeno-free (Xf) culture system. (A) Human iPSCs established from skin-derived primary fibroblasts (987A3 and 987A7), peripheral blood-derived T-cells (1027B3 and 1027B6), peripheral blood-derived non-T-cells (1120C7 and 1120C12) and cord blood cells (1156D2 and 1156D15) under the Ff and Xf culture system. Photographs were taken between passages p5 and p10. Scale bar, 100 μm. (B) The gene expression levels of pluripotency markers as determined using RT-PCR. "LN" indicates that the cells were cultivated using the Ff and Xf culture system reported herein. "Feeder" indicates cells that were cultivated on murine feeders with non-Xf medium. (C) The growth curve of the feeder-free iPS cells cultured under Ff and Xf culture conditions.

chain, substitution of which with glutamine abolishes the integrin binding activity of LN511E8[24], in our culture method using an EQ mutant of rLN511E8. The colony formation of 201B7 was not observed on EQ mutant-coated plate (Figure S5).

Recently, the defined and simplified Xf medium, E8, was reported[13]. The major difference in formulation between E8 and StemFit™ is albumin. StemFit™ includes human albumin (E8 does not include any albumins). Albumin has many biological and

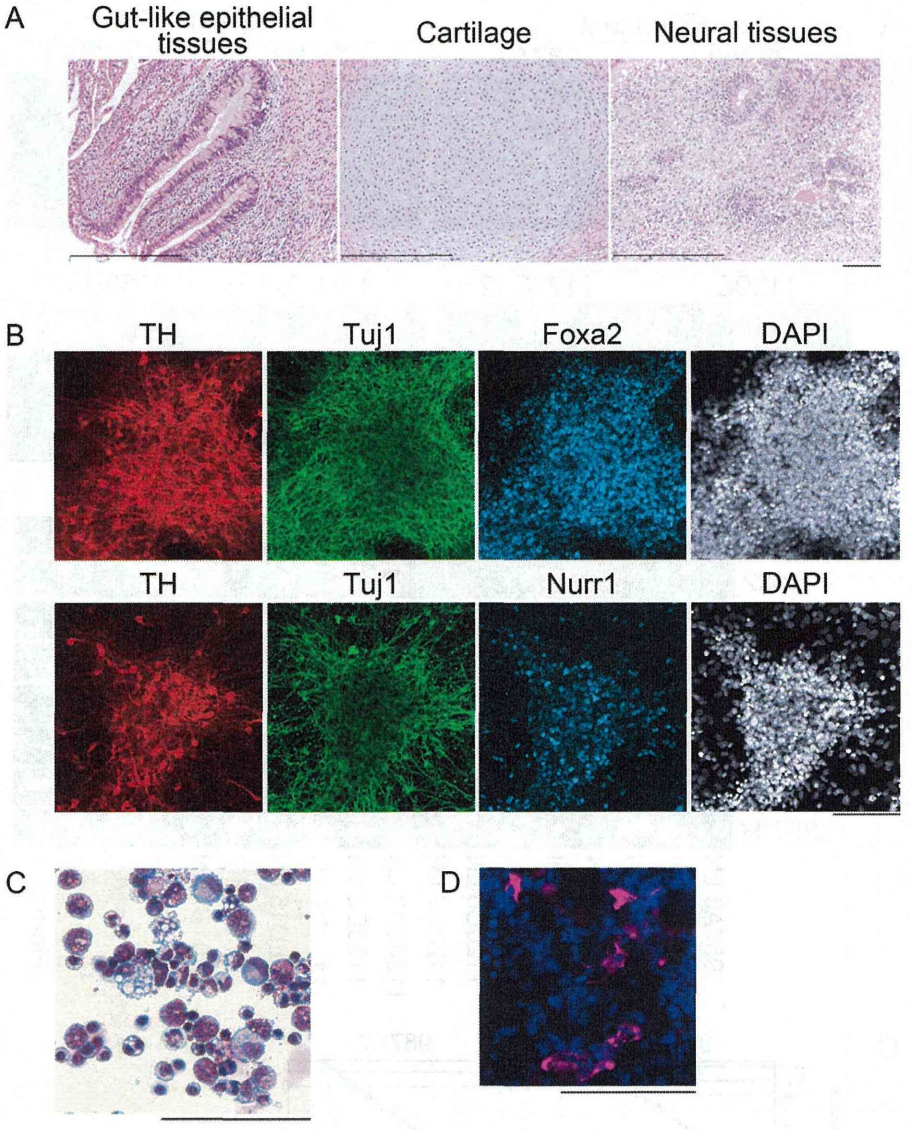

Figure 3 | The differentiation capacity of the T-cell-derived feeder-free hiPSC clone, 1027B6 (p7–p12). (A) Hematoxylin and eosin staining of teratomas showing representative derivatives of all three germ layers. Scale bar, 100 μm. (B) Differentiation into mesencephalic dopaminergic neurons under Xf conditions. Photomicrographic images of immunostaining for Tuj1 (green), tyrosine hydroxylase (TH: red), Foxa2 or Nurr1 (blue) and DAPI (white). Scale bar, 100 μm. (C) May-Grünwald-Giemsa staining of differentiated blood cells on day 16 showing hematopoietic precursor cells, myeloid precursor cells, macrophages and erythroblasts. Scale bar, 100 μm. (D) Feeder-free hiPSCs differentiated into insulin-producing cells. After 23 days of culture under the differentiation conditions, the cells were fixed and stained with Hoechst33342 (blue) and anti-insulin antibodies (magenta). Scale bar, 100 μm.

physical roles. Thus, this factor may confer difference in performance between the both.

We are planning to build up a bank of hiPSCs for transplantation therapy. The human leukocyte antigen (HLA) is a key factor that mediates the immune-related rejection after transplantation. To minimize the immune system-related rejection, it is necessary to match the HLA type of the donor and recipient. Matching the HLA type is difficult because of the large number of HLA types present in each individual. However, the Japanese population is relatively homogeneous compared to other populations, and it has been reported that 50–140 HLA-homozygous cell lines would match 90% of the Japanese population[17,22], a HLA-homozygous hiPSC bank would therefore be a helpful resource for therapeutic application in Japan.

Ensuring the quality and safety of hiPSC are important for their clinical application. Manufacturing hiPSCs should be performed in the Cell Processing Center under the GMP guidelines. Our novel hiPSC culture system is comparable to that of standard cell lines, such as 293 cells or HeLa cells, making previously complex steps more routine. Employing this easy to use, reproducible and expandable culture system, a large amount of clinical-grade hiPSC stock can be made at early passage numbers at the same time. Moreover, the procedures needed to establish and maintain Ff-hiPSCs should be minimal and simple in the CPC. In order to apply Ff-hiPSCs for clinical applications, it is necessary to reduce or completely eliminate the use of animal-derived materials. To achieve this, we selected the StemFit™ medium, which does not contain animal-derived materials. This culture system is a promising method for manufacturing clinical-grade hiPSCs. In addition, it is necessary to use defined culture system for the source of iPS cells, such as fibroblasts or blood cells[13,23].